Synthesis of Duplexers With the Common Port Matched at All Frequencies

Stefano Tamiazzo and Giuseppe Macchiarella, *Senior Member, IEEE*

I. Introduction

DUPLEXERS are three-port selective networks, mainly used for connecting a single antenna to the transceiver of a communication system (with the receiving and transmitting bands more or less close together). They are typically constituted by two filters, whose inputs are connected to the first port (referred to as the *antenna port*) through a suitable three-port network (referred as the *junction*); the outputs of the filters are the other two ports of the duplexer (*TX port* and *RX port*). In the simplest type of duplexer, the junction is realized by means of a nonreciprocal three-port (circulator); in this way the interaction between the two filters is removed and the design of the duplexer reduces to that of two filters taken separately. This solution, however, is not always possible or convenient, for several reasons (cost, additional unwanted effects, etc.), so several approaches to the design of duplexers employing a reciprocal three-port junction have been developed [1]–[4]. Anyhow, all of them assume the classical topology of the duplexer recalled above, i.e., two filters connected through a three-port reciprocal junction. Recently, some works have appeared in the literature [5], [6] that suggest a more general representation of the duplexer, which is assumed to be a three-port lossless network, composed of resonators arbitrarily coupled to each other, without any specific constraint about the topology. In other words, it is currently being investigated if some advantages are possible abandoning the constraint imposed by the classical duplexer topology. Actually, this is still an open question because a general solution allowing to specify arbitrary transmission characteristics between the antenna port and the two output ports of the duplexer has not yet been conceived with an arbitrary three-port network (due also to the difficulties of exploiting the unitary conditions of the scattering matrix in arbitrary three-port lossless networks [7]).

Manuscript received May 31, 2013; revised October 31, 2013; accepted October 31, 2013. Date of publication November 26, 2013; date of current version January 06, 2014.

S. Tamiazzo is with Commscope Italy, Agrate Brianza 20090, Italy (e-mail: stefano.tamiazzo@commscope.com).

G. Macchiarella is with the Dipartimento di Elettronica, Informazione e Bioingegneria, Politecnico di Milano, 20133 Milan, Italy (e-mail: giuseppe.macchiarella@polimi.it).

In this paper, we propose a solution for a class of duplexers synthesized as a generic three-port lossless network with the antenna port matched at all frequencies. This duplexer was originally implemented by means of complementary low-pass–high-pass filters, connected in parallel at the input port [8]. The most common way to realize today this kind of duplexer is, however, based on a directional structure, which is composed by two identical filters connected through two 90° hybrids [9]. Some recent works have proposed a design approach that incorporate the hybrids into the coupled resonators structure [10], [11]. Here, we present another approach to the design of this kind of duplexer, based on polynomial modeling of a three-port network composed of coupled resonators (transformed into a low-pass normalized frequency domain [12]). Note that, unlike the previous design approaches (which assume the duplexer as a four-port network, with one port terminated on a matched load), our approach considers a true three-port network without any additional matched termination. Furthermore, our duplexer does not require the 90° hybrids of the classical configuration.

This paper is organized as follows. Section II presents the theory behind the design approach adopted. Section III describes the synthesis of the transversal canonical prototype for three-port networks. In Section IV, a suitable transformation of the canonical prototype is presented in order to get a topological configuration more convenient for a practical implementation than the transversal one. Section V shows the validation of the proposed approach by means of the design and fabrication of a test device. Conclusions are presented in Section VI, followed by an Appendix where the algorithm devised for the generation of a family of canonical prototypes for three-port networks (used in Section IV) is presented.

II. Polynomial Modeling of the Three-Port Network

A generic duplexer can be represented, for synthesis purposes, as a three-port, reciprocal, and lossless network (Fig. 1).

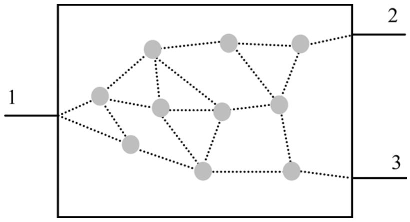

Fig. 1. General schematization of the selective three-port network here considered (duplexer). The grey circles and the dashed lines represent the cavities and the coupling structures, respectively.

We assume that the network in Fig. 1 is composed of resonant cavities arbitrarily coupled to each other (with some of them also coupled to the three ports). As usually done in the synthesis of microwave filters based on the equivalence with a lumped network [12], each cavity is represented in a specified low-pass frequency domain by means of a lumped capacitor of unit value in parallel with a frequency-invariant susceptance, while the couplings are modeled with frequency-invariant admittance inverters. Note that this is an approximation of the physical reality, which typically produces satisfactory results only in a small or moderate frequency interval.

Under the above assumptions, the scattering matrix elements of the three-port network in Fig. 1 can be represented as the ratio of polynomials in the normalized complex variable s (which is related to the real frequency domain through the well-known low-pass-to-bandpass frequency transformation [12])

$$\mathbf{S} = \{s_{i,j}\} = \frac{1}{e(s)}\{g_{i,j}(s)\}. \tag{1}$$

Note that the roots of $e(s)$ represent the N poles of the three-port.

The lossless condition implies the following relations among the polynomials $g_{i,k}$ and e:

$$\begin{aligned} &\sum_{k=1,3} g_{i,k} \cdot g^*_{i,k} = e \cdot e^*, \\ &\sum_{k=1,3} g_{i,k} \cdot g^*_{j,k} = 0, \qquad i,j = 1,2,3\ (i \neq j) \\ &\det\left(\left\{\frac{g_{i,j}}{e}\right\}\right) = \frac{\Theta^*(s)}{\Theta(s)} \end{aligned} \tag{2}$$

where $\Theta(s)$ is a polynomial depending on the network topology. The superscript asterisk $(^*)$ define the para-conjugate operator [12].

Due to the reciprocity, the distinct polynomials are actually seven; they will be referred in the following as:

$$\begin{aligned} g_{11} &= F_1(s) \\ g_{22} &= F_2(s) \\ g_{33} &= F_3(s) \\ g_{12} = g_{21} &= P_2(s) \\ g_{13} = g_{31} &= P_3(s) \\ g_{32} = g_{32} &= I(s) \\ e &= E(s). \end{aligned} \tag{3}$$

Concerning the degree of these polynomials, it can be said that the lossless condition alone does not imply that the order of $E(s)$ is necessarily equal to the number N of cavities in the duplexer. In practice, however, the ordinary implementations of duplexers always exhibit this property. A way to impose N equal to the number of cavities is to assume the following condition on the determinant of the scattering matrix:

$$\det\left(\left\{\frac{g_{i,j}}{e}\right\}\right) = \frac{E^*(s)}{E(s)} \Rightarrow \Theta(s) = E(s). \tag{4}$$

Introducing this condition in (2), after some algebraic manipulations the following equations can be found (the dependence of all the polynomials on s is implicitly assumed):

$$\begin{aligned} F_1F_2 &= P_2^2 + EF_3^* \\ F_1F_3 &= P_3^2 + EF_2^* \\ F_2F_3 &= I^2 + EF_1^* \\ P_2P_3 &= F_1I + EI^* \\ P_3I &= F_2P_2 + EP_2^* \\ P_2I &= F_3P_3 + EP_3^*. \end{aligned} \tag{5}$$

Note that there is no explicit solution for the polynomials from the above equations. This fact has an important consequence: we cannot assign a transmission and/or reflection characteristic to a three-port reciprocal and lossless network independently on the topology of the network (as instead it is possible with the classical two-port filters).

In this paper, we have then imposed an additional constraint, which allows to get an explicit solution for the polynomials in (5). Such a constraint consists of assuming the antenna port of the duplexer matched at all frequencies, i.e., $S_{11} = 0$, and therefore, $F_1 = 0$.

Note that the class of duplexers so identified (referred to as *matched duplexers*) has been known for a long time [9] and is of particular interest in many practical applications. A matched duplexer is usually implemented by means of two identical filters connected through two 90° hybrids [9]. Recently, these devices have been proposed for realizing reconfigurable combiners, and some works have illustrated design approaches based on synthesis techniques [10], [11]. The design approach described here allows the realization of matched duplexers that do not need hybrids.

For deriving explicitly the polynomials in the considered case (i.e., $F_1 = 0$), we assume, first of all, that the degree N of $E(s)$ is even; it is then possible to make the following assumptions concerning the polynomials F_2, F_3, and E:

$$F_2(s) = k_2^2R^2(s) \quad F_3(s) = k_3^2T^2(s) \quad E(s) = W^2(s) \tag{6}$$

with $R(s)$ and $T(s)$ monic polynomials of degree N_R and N_T, respectively, whose roots are imposed to be on the imaginary axis. We also assume that the coefficient k_2 and k_3 are real or imaginary numbers (the highest degree coefficient of F_2 and F_3 is anyhow real). N_R is assumed equal to the degree of the polynomial W, given by $N_W = N/2$, and N_T must be lower than or equal to N_W. Note that these assumptions imply N to be even.

Introducing (6) into (5) with $F_1 = 0$ and taking into account (2), the following results are obtained:

$$P_2(s) = jk_2 W(s) \cdot R^*(s) \tag{7}$$
$$P_3(s) = jk_3 W(s) \cdot T^*(s) \tag{8}$$
$$I(s) = -k_2 k_3 R(s) \cdot T(s) \tag{9}$$
$$W(s) \cdot W^*(s) = k_2^2 R(s) \cdot R^*(s) + k_3^2 T(s) \cdot T^*(s). \tag{10}$$

Equations (7)–(10) suggest that the polynomials $T(s)$ and $R(s)$ can be obtained from the synthesis of a two-port filter with assigned transmission $(k_3 \cdot T(s)/W(s))$ and reflection $(k_2 \cdot R(s)/W(s))$ characteristics. The synthesis can be carried out with one of the methods available in the literature [12], by assigning the order N_W to the filter together with the return loss (determining the attenuation in band 1) and the imaginary transmission zeros represented by the roots of polynomial T (that determine the attenuation in band 2). Note that the highest degree coefficients of the reflection and transmission polynomials coming from the synthesized filter represent the coefficients k_2 and k_3. With this assignment, the transmission parameters of the duplexer (S_{21} and S_{31}) become equal (in magnitude) to the transmission and reflection of the two-port filter

$$S_{21} = \frac{P_2(s)}{E(s)} = jk_2 \frac{R^*(s)}{W(s)}$$
$$S_{31} = \frac{P_3(s)}{E(s)} = jk_3 \frac{T^*(s)}{W(s)}. \tag{11}$$

The isolation (S_{23}) and the output ports matching (S_{22}, S_{33}) result,

$$S_{22} = \frac{F_2(s)}{E(s)} = k_2^2 \left(\frac{R(s)}{W(s)}\right)^2$$
$$S_{33} = \frac{F_3(s)}{E(s)} = k_3^2 \left(\frac{T(s)}{W(s)}\right)^2$$
$$S_{23} = -k_2 k_3 \frac{T(s)R(s)}{W^2(s)}. \tag{12}$$

Note that isolation between ports 2 and 3 is assured by the zeros on imaginary axis in T and R. The output ports matching is also somehow enhanced by the multiple zeroes of T^2 and R^2, respectively.

To illustrate the polynomials evaluation introduced above, let consider a duplexer with the following requirement (in the normalized frequency domain).

- Band 1: $[-1, 1], N_R = 4$, attenuation in band 2: 21 dB.
- Band 2: $[1.135, 3.5], N_T = 2$, attenuation in band 1: 21 dB.

The polynomials T, R and W are obtained from the synthesis of a two-port filter exhibiting an equi-ripple response in the passband and stopband (attenuation and return loss equal to 21 dB). In order to get this goal, two transmission zeros have been imposed on the imaginary axis at 1.4846 and 1.1582.

The roots of polynomials T, R, and W, obtained from the polynomials of the two-port filter, as explained above, are reported in the following, together with the coefficients k_1 and k_2.

- Roots of R: $[-0.8389i, 0.9797i, 0.7563i, 0.0642i]$.
- Roots of T: $[1.4846i, 1.1582i]$.

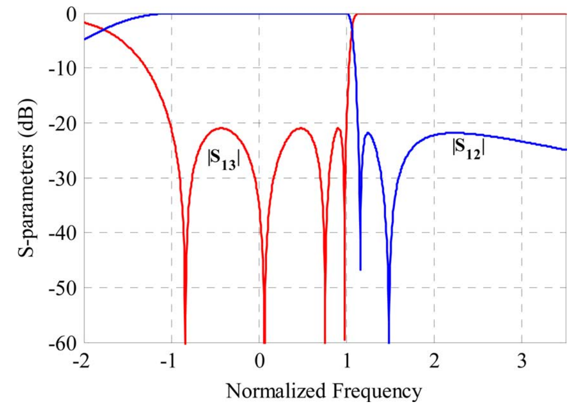

Fig. 2. Transmission responses of the duplexer in example.

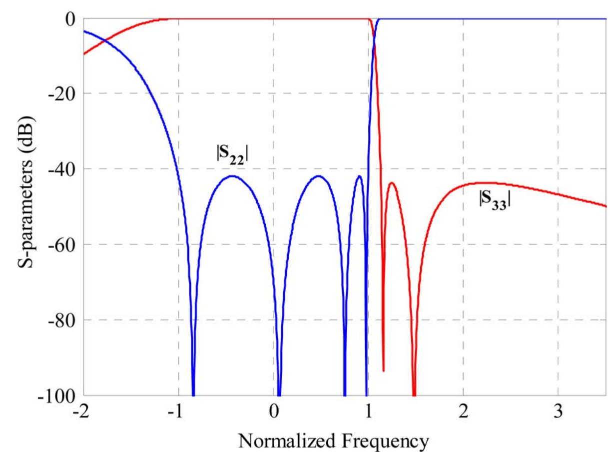

Fig. 3. Output ports matching of the duplexer in example.

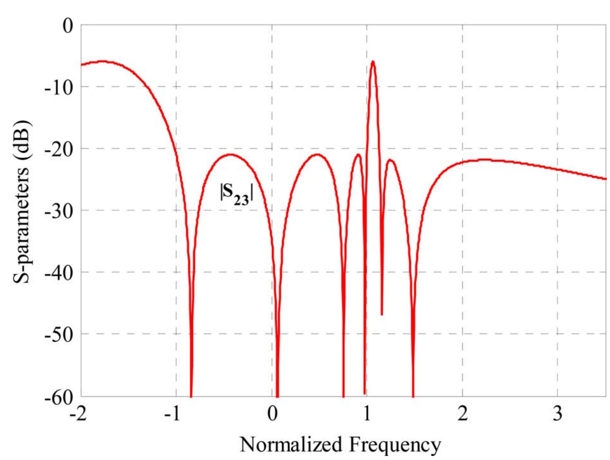

Fig. 4. Isolation of output ports of the duplexer in example.

- Roots of W: $[-0.82601 - 1.4217i, -1.1058 + 0.31331i, -0.33789 + 1.0076i, -0.058084 + 1.062i]$.

$k_2 = 1$ and $k_3 = 1.2420i$.

Figs. 2–4 show the transmission, reflection, and isolation of the duplexer characterized by the computed polynomials.

III. Synthesis of the Prototype Three-Port Network

Once the polynomials defining the desired response have been defined, the next step of the design is the synthesis of a

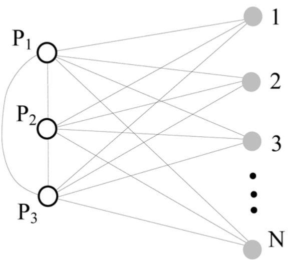

Fig. 5. Transversal prototype canonical network for a three-port network. The dashed line represent the admittance inverters $J_{m,n}$ and the gray nodes are unit capacitances in parallel to the susceptances b_m. Also the couplings among the ports are represented with ideal inverters ($J_{0m,n}$). It is assumed that a susceptance B_{0k} may appear also in parallel to the port P_k.

prototype network in the normalized frequency domain. As explained in the previous section, we assume that this network is composed of unit capacitances in parallel with frequency invariant susceptances, coupled to each other with ideal admittance inverters.

Even if very few works are available in the literature on multiport synthesis, the classical transversal canonical prototype introduced in [13] for two-port filters has been recently generalized to an arbitrary multiport network [5]. Such a prototype, in case of a three-port network, assumes the form shown in Fig. 5.

Using the same formalism adopted in [5], we introduce the following normalized coupling matrix $\mathbf{M}$ defining the above network:

$$\mathbf{M} = \begin{bmatrix} B_{01} & J_{021} & J_{031} & J_{11} & \cdots & J_{N1} \\ J_{021} & B_{02} & J_{032} & J_{21} & \cdots & J_{N2} \\ J_{031} & J_{032} & B_{03} & J_{31} & \cdots & J_{N3} \\ J_{11} & J_{21} & J_{31} & b_1 & 0 & 0 \\ \vdots & \vdots & \vdots & 0 & \ddots & 0 \\ J_{N1} & J_{N2} & J_{N3} & 0 & 0 & b_N \end{bmatrix}. \quad (13)$$

Note that the order of $\mathbf{M}$ is $N+3$; the first three rows and columns refer to the couplings involving the ports.

The elements of the $\mathbf{Y}$ matrix of the transversal prototype are readily derived from $\mathbf{M}$, taking into account that all the capacitors in the network have unit value [it is assumed in (14) $i = 1,2,3$ and $n,m = 1,2,3$ $(n \neq m)$]

$$y_{ii} = jB_{0i} + \sum_{k=1}^{N} \frac{J_{ik}^2}{s + jb_k}$$
$$y_{nm} = jJ_{0nm} + \sum_{k=1}^{N} \frac{J_{nk}J_{mk}}{s + jb_k}. \quad (14)$$

The $\mathbf{Y}$ matrix whose elements are reported in (14) must be now equated to the admittance matrix defined by the duplexer polynomials introduced in the previous section. For deriving this latter matrix, we apply the well-known relationship between $\mathbf{S}$ and $\mathbf{Y}$ matrices

$$\mathbf{Y} = (U_3 - \mathbf{S})(U_3 + \mathbf{S})^{-1} = \frac{1}{d} \begin{bmatrix} n_{11} & n_{21} & n_{31} \\ n_{21} & n_{22} & n_{32} \\ n_{31} & n_{32} & n_{33} \end{bmatrix} \quad (15)$$

where d and n_{ij} are all polynomials. Note that, with the assumptions of Section II, it can be stated that the order of polynomial d is less than or equal to N.

Using (15) and (5) with $F_1 = 0$, the following expressions can be written for the elements of $\mathbf{Y}$:

$$\begin{aligned} n_{11} &= (E - E^*) + (F_2 - F_2^*) + (F_3 - F_3^*) \\ n_{22} &= (E - E^*) - (F_2 - F_2^*) + (F_3 - F_3^*) \\ n_{33} &= (E - E^*) + (F_2 - F_2^*) - (F_3 - F_3^*) \\ n_{21} &= -2(P_3 - P_3^*) \\ n_{31} &= -2(P_2 - P_2^*) \\ n_{32} &= -2(I - I^*) \\ d &= (E + E^*) + (F_2 + F_2^*) + (F_3 + F_3^*). \end{aligned} \quad (16)$$

It is possible to put the elements $y_{ij} = n_{ij}/d$ in the form (14) by expanding the ratios n_{ij}/d as follows:

$$y_{ij} = \frac{n_{ij}}{d} = K_{ij} + \sum_{k=1}^{N} \frac{r_{ij,k}}{s - p_k}. \quad (17)$$

In (17), p_k represents the kth roots of $d(s)$ (imaginary), K_{ij} and $r_{ij,k}$ are the constant term and the residues of the root p_k, respectively, in the expansion of the term n_{ij}/d. Furthermore, the following relations among the residuals $r_{ij,k}$ hold true for each $k = 1, \ldots, N$:

$$\begin{aligned} r_{11,k} r_{22,k} &= r_{21,k}^2 \\ r_{22,k} r_{33,k} &= r_{32,k}^2 \\ r_{11,k} r_{33,k} &= r_{31,k}^2 \\ \mathrm{sgn}(r_{21,k} r_{31,k}) &= \mathrm{sgn}(r_{32,k}). \end{aligned} \quad (18)$$

Again, it can be shown that the conditions (18) are a consequence of (5), provided that the roots of d are simple (if there are multiple roots in d, the synthesis of the transversal prototype with this method is no more possible).

Equations (14) and (17) can be equated term by term, provided that relations (18) hold true, resulting in the following explicit expressions, valid for $k = 1, \ldots, N$ and $n, m = 1, 2, 3$ $(n \neq m)$:

$$\begin{aligned} J_{1k} &= \sqrt{r_{11,k}} \\ J_{2k} &= \mathrm{sgn}(r_{21,k}) \sqrt{r_{22,k}} \\ J_{3k} &= \mathrm{sgn}(r_{31,k}) \sqrt{r_{33,k}} \\ jJ_{0nm} &= K_{nm} \\ jb_k &= -p_k \\ jB_{0n} &= K_{nn}. \end{aligned} \quad (19)$$

It should be noted that the lossless property implies that all K_{mn} and p_k are purely imaginary while all $r_{ij,k}$ are real ($r_{ii,k}$ positive and real). This assures that the parameters J, b and B are all real. The square roots in (19) are assumed to be all positive.

To verify the above procedure for building up the transversal three-port canonical prototype, the polynomials computed in Section II have been used for synthesizing a duplexer with matched antenna port. The evaluated coupling matrix $\mathbf{M}$ is shown at the bottom of this page. The response of the three-port network, computed through $\mathbf{M}$, is not here reported because it coincides with the one obtained through the polynomials, already shown in Figs. 2–4.

IV. Topologic Transformation

The use of the canonical transversal prototype is impractical in most applications so we have investigated various techniques for transforming the coupling matrix. As a result, an original procedure has been devised for generating a family of canonical prototypes, starting from the matrix of the transversal one (the procedure is illustrated in the Appendix). Using this procedure, we realized that if specific conditions on the assigned polynomials are met, the matched duplexer can be implemented with a very simple and convenient configuration.

The necessary conditions regarding the characteristic polynomials are the following.

- The degrees N_T and N_R of the polynomials T and R, respectively, must obey

$$N_T \leq N_R - 2. \tag{20}$$

- The sign of the highest degree coefficients of polynomials F_2 and F_3 must satisfy

$$\text{sign}\left(F_3^{(m)} \cdot (i)^m\right) = -\text{sign}\left(F_2^{(n)} \cdot (i)^n\right) \tag{21}$$

  where m and n are the degree of F_3 and F_2, respectively, and i is the imaginary unit.

We can observe that the previous rules are easily met when the polynomials of the duplexer are obtained from the synthesis of a two-port filter, as explained in Section II. It is, in fact, sufficient to impose $nz \leq np - 2$ with nz number of transmission zeros and np number of poles in this filter. The second is implied by the imaginary unit multiplying the highest degree coefficient of the transmission polynomial of the synthesized filter when the difference np-nz is even [14].

Duplexers satisfying the above conditions can be implemented with the topology shown in Fig. 6.

It can be demonstrated that this topology (Fig. 6), even if not strictly canonical, can be found among the ones generated with the algorithm reported in the Appendix, provided the conditions (20) and (21) are met. On the other hand, its identification among all the ones obtained with the mentioned algorithm is not at all an easy task, considering the inevitable need to renumber the nodes. Therefore, it may be more convenient, from a computational point of view, to generate such a topology with the method based on the optimization of the rotation angles [16] recalled in the Appendix.

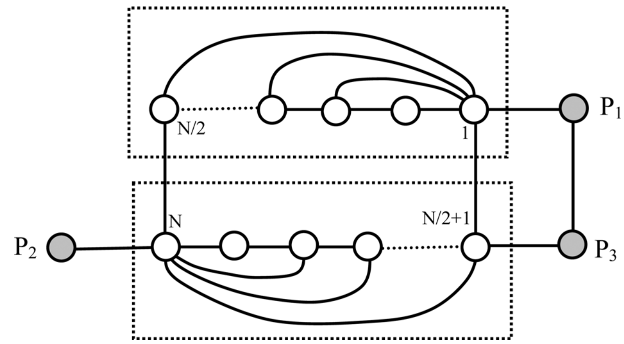

Fig. 6. General topology for the matched duplexer. Port 1 is the matched common node.

You can also observe that the two-port subnetworks inside the dashed boxes have an arrow topology and can therefore be reconfigured to a more convenient topology (from a practical point of view), using the well-known sequence of rotations used for two-port filters [15].

To test the proposed topologic transformation, the matched duplexer considered in Section III has been synthesized in the form of Fig. 6. The configuration obtained (with the computed elements of the coupling matrix) is reported in Fig. 7. The transformed matrix has been obtained with the optimization of the rotation angles. We have also verified that it belongs to the family of canonical prototypes generated by the algorithm reported in the Appendix: in fact, the same topology is obtained by applying this algorithm with $N = 8$, $c =$ '0002212' and $p = 3$.

As already observed, the topology generated by the algorithm (reported for reference in Fig. 8) has a different nodes numbering with respect to the expected one (Fig. 6) so its automatic identification among all the ones produced by the algorithm may be problematic.

Observing the scheme in Fig. 8, one can note that, other than the numbering of the nodes, the signs of some couplings are also

0	0	−1	0.6962	0.6889	0.552	0.1204	0.3278	0.7533	0.5232	0.3118
0	0	0	0.6962	0.6889	−0.552	−0.1204	0.3278	−0.7533	−0.5232	0.3118
−1	0	0	−0.6962	0.6889	0.552	−0.1204	0.3278	−0.7533	0.5232	−0.3118
0.6962	0.6962	−0.6962	2.4279	0	0	0	0	0	0	0
0.6889	0.6889	0.6889	0	−1.6570	0	0	0	0	0	0
0.552	−0.552	0.552	0	0	−1.5997	0	0	0	0	0
0.1204	−0.1204	−0.1204	0	0	0	−1.0727	0	0	0	0
0.3278	0.3278	0.3278	0	0	0	0	−0.8812	0	0	0
0.7533	−0.7533	−0.7533	0	0	0	0	0	0.8614	0	0
0.5232	−0.5232	0.5232	0	0	0	0	0	0	0.8499	0
0.3118	0.3118	−0.3118	0	0	0	0	0	0	0	−0.8499

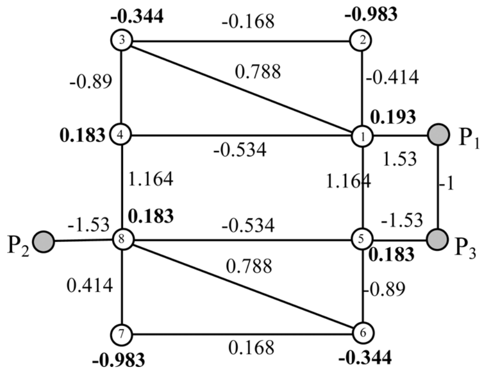

Fig. 7. Matched duplexer with the transformed topology. The numbers represent the coupling matrix elements (those in bold are the main diagonal elements).

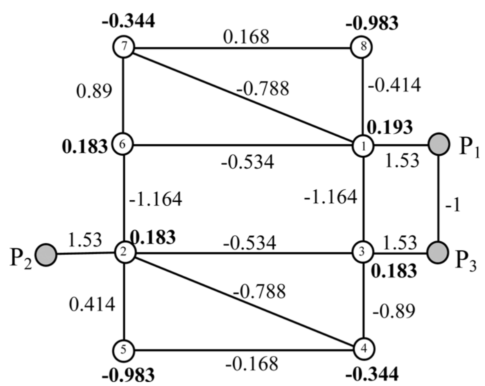

Fig. 8. Matched duplexer topology obtained with the algorithm reported in the Appendix. Note that the numbering of nodes is different with respect to Fig. 7. The sign of some couplings is also reversed.

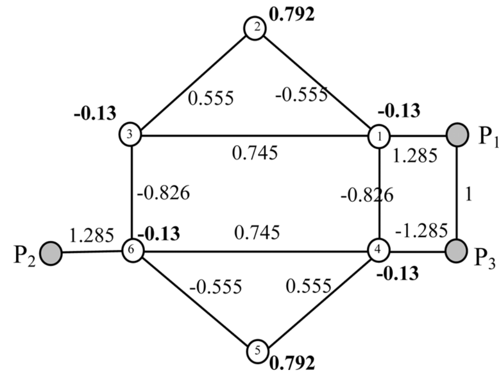

Fig. 9. Scheme of the test duplexer. The numbers represent the elements of the coupling matrix.

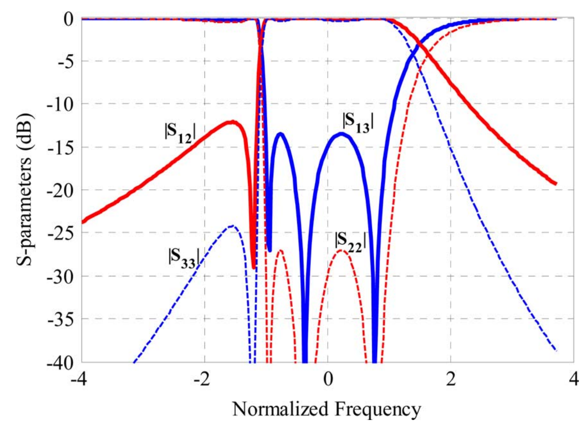

Fig. 10. Response of the matched duplexer in the normalized domain.

different with respect to the corresponding ones in Fig. 7. This means that there may exist topologies with couplings differing only for some signs that present the same response (with possibly a different constant phase term).

V. Experimental Validation

To validate the proposed design approach, a matched duplexer was designed and fabricated. The following electrical specs have been imposed.

- Band 1: 2138.2–2155.8 MHz.
- Band 2: 2120–2135 MHz.
- Attenuation of channel 1 in band 2: >12 dB.
- Attenuation of channel 2 in band 1: >13 dB.
- Return loss at all ports: >20 dB.

The normalized frequency domain used for the synthesis of the normalized prototype is defined by the usual bandpass-lowpass frequency transformation

$$w = \frac{B}{f_0}\left(\frac{f}{f_0} - \frac{f_0}{f}\right) \tag{22}$$

with f_0 and B obtained by imposing the mapping of the normalized frequencies -1 and 1 to the initial and final frequencies of band 1 (2138.2 and 2155.8 MHz, respectively). It has $B = 17.6$ MHz and $f_0 = 2146.982$ MHz.

The synthesis of the normalized prototype starts with the definition of the reference two-port filter. A filter of order 3 with one transmission zero can meet the specs. The following assignments have been then used:

$$np = 3,\ \mathrm{RL} = 13.5\ \mathrm{dB},\ w_z = -1.2055$$

where w_z represents the normalized frequency of the transmission zero.

The evaluation of the coupling matrix $\mathbf{M}$ has been carried out according to the procedure of Section IV. Fig. 9 shows the scheme of the prototype network obtained by the synthesis, together with the elements of the coupling matrix. The computed response in the normalized frequency domain of this three-port network is reported in Fig. 10.

The next step of the design is the de-normalization of the prototype, performed through the following expressions [14]:

$$\begin{aligned} Q_{p,m} &= \frac{f_0}{B}\frac{1}{M_{p,m}^2} \\ k_{i,j} &= \frac{B}{f_0} M_{i,j} \\ f_{ris,q} &= f_0\left[\sqrt{1+\left(\frac{B}{f_0}\frac{M_{q,q}}{2}\right)^2} - \left(\frac{B}{f_0}\frac{M_{q,q}}{2}\right)\right] \end{aligned} \tag{23}$$

where $Q_{p,m}$ represents the external Q of resonator m coupled to the port p; $k_{i,j}$ is the coupling coefficient of the coupled resonators (i,j); $f_{ris,q}$ is the resonant frequency of resonator q.

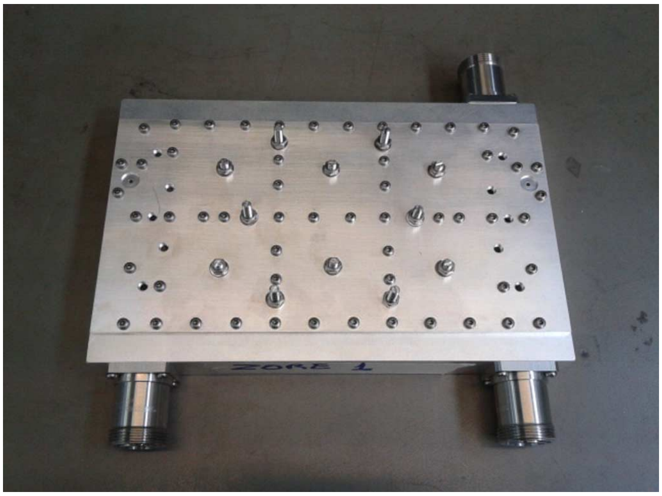

Fig. 11. Photograph of the body of the matched duplexer. The tuning screws are visible on the cover of the structure.

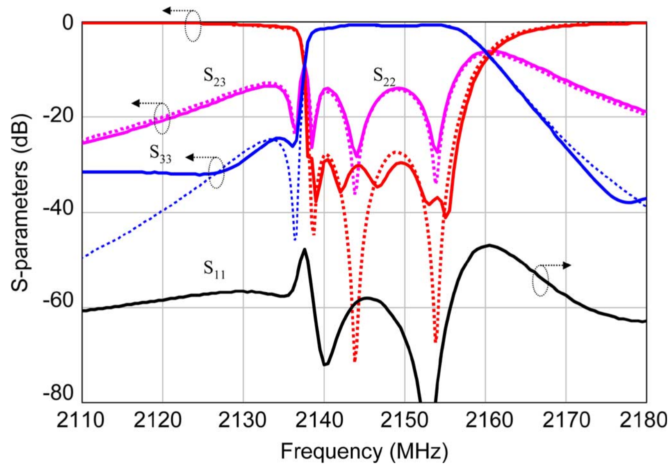

Fig. 12. Response of fabricated duplexer. Solid lines refer to the measurements, dashed lines to the simulations (performed with the de-normalized equivalent circuit). S_{22} and S_{33} represent the return loss at ports 2 and 3; S_{23} is the isolation between the output ports (2, 3); S_{11} is the return loss at the common port (the simulated curve is not reported because the simulated matching is larger than -100 dB at all frequencies).

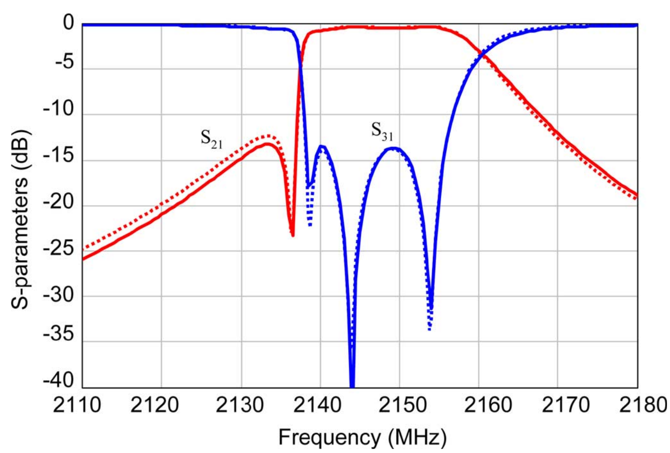

Fig. 13. Response of fabricated duplexer (continued). S_{21} and S_{31} are the transmission between the common port (1) and the output ports (2, 3).

The following results are obtained from (23) (f_{ris} are in megahertz):

$$Q_{1,1} = Q_{2,6} = 73.9$$
$$Q_{3,4} = -73.9$$
$$k_{1,2} = -0.0046$$
$$k_{1,3} = 0.0061$$
$$k_{1,4} = -0.0068$$
$$k_{2,3} = 0.0046$$
$$k_{3,6} = -0.0068$$
$$k_{4,5} = 0.0046$$
$$k_{4,6} = 0.0061$$
$$k_{5,6} = -0.0046$$
$$f_{ris} = [2148.12, 2140.02, 2148.12, 2148.12, 2140.02, 2148.12].$$

Note that there is also a unit coupling between ports 1 and 3; it consists, in the de-normalized domain, of an ideal inverter with the same impedance of the ports.

The last step of the design is the selection and dimensioning of suitable cavities implementing the resonators in the de-normalized frequency domain. The duplexer considered here has been conceived for the base stations of mobile communications, where coaxial cavities with capacitive loading (for reducing the overall size) are typically adopted. The size of the cavities has been selected to get an unloaded Q of about 5000, which is obtained with the following assignments: side $=$ 55 mm, height $=$ 30 mm, inner rod diameter $=$ 15 mm. The direct coupling between ports 1 and 3 is realized with a transmission line a quarter-wavelength long and with 50-Ω characteristic impedance (that approximates the ideal inverter mentioned before). The main couplings are implemented by opening windows of suitable size between the coupled cavities; for the cross couplings, probes with suitable dimensions have been used. The coupling with the external ports is realized by means of a tap on the inner conductor of the involved cavities.

The dimensioning of all the couplings has been carried out by considering two cavities at a time and applying the well-known technique based on the even and odd resonance frequencies ([11, Ch. 14]). The conventional CNC milling has been used for fabricating the body of the duplexer. Screws have been included in the cover for allowing the accurate tuning of the cavities and couplings. A photograph of the fabricated device in shown in Fig. 11.

The measured response of the aligned duplexer is reported in Figs. 12 and 13; for comparison, the response obtained by simulating the de-normalized equivalent circuit of the duplexer with a commercial circuit simulator is also reported on the figures (the unloaded Q of resonators was set to 5000). Note that the matching at the antenna port ($|S_{11}|$ in Fig. 12) is limited by the fabrication tolerances; it remains anyhow better than -30 dB in both the passbands. Overall, we can say that there is an excellent agreement between the measurements and simulations.

VI. Conclusion

In this paper, a novel approach to the design of a duplexer with the antenna port matched at all frequencies has been presented. The method described is based on the polynomial characterization of the duplexer, which is assumed as a generic three-port lossless network composed of arbitrarily coupled resonators. In addition to the design procedure, two other interesting achievements have been here presented.

- The derivation of the characteristic polynomials of a three-port network by imposing: the lossless condition (unitary scattering matrix S), the condition (4) on the determinant of S, and the polynomial at numerator of S_{11} identically zero
- The sequence of matrix rotations defining a general family of canonical prototypes, starting from the transversal one.

Regarding the configuration of the matched duplexer here developed, it must be noted that it represents the first solution with an actual three-port network (i.e., not belonging to the classical four-port configuration with two identical filters and two 90° hybrids).

The design procedure has been validated by the realization of a test device, whose measurements have proven to be in excellent agreement with the expectations.

To conclude, it is also worth mentioning the limitations of the proposed solution. First of all, it must be said that the actual matching at the input port depends on the degree of symmetry of the implemented network. In practice, a return-loss level larger than 30 dB can hardly be achieved. Another drawback respect the classical four-port configuration (that uses 90° hybrids) is represented by the finite isolation between the output ports that cannot be specified independently by the transmission parameters S_{21} and S_{31} (it is, in fact, proportional to their product). Being, however, that S_{21} and S_{31} are reciprocal to each other (they represent the transmission and the reflection of the reference filter, respectively), the isolation is expected to also be sufficiently small in the proposed duplexer configuration.

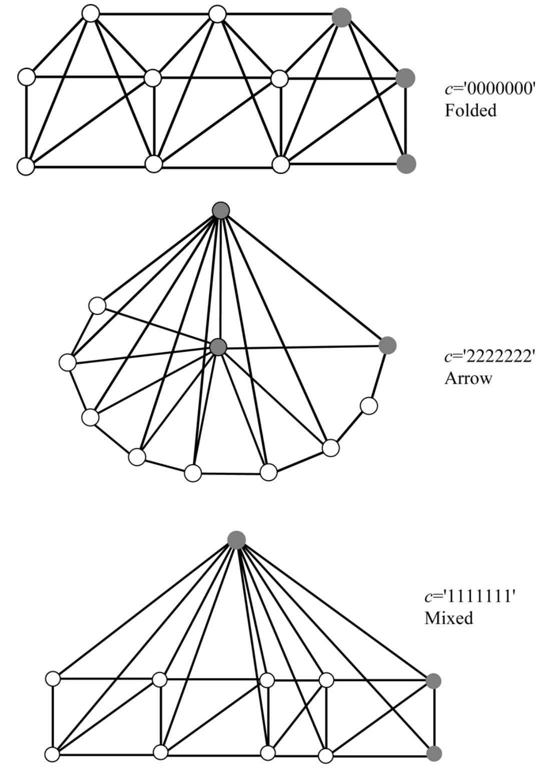

Fig. A1. Three canonical topologies obtained with the developed algorithm for $p = 3$ and $N = 8$. The grey nodes represent the ports. Note that several couplings in the above drawings may disappear (i.e., their resulting value is zero), depending on the polynomials originally assigned for the synthesis of the transversal prototype used as starting point by the proposed algorithm.

APPENDIX

Here, the derivation of a general algorithm for generating a class of canonical topologies for p-port networks is presented.

Let assume that the considered network belongs to the class defined in Fig. 1 (Section II), where the scattering matrix at the p ports is defined through suitable characteristic polynomials. We assign the term *canonical* to all the specific topologies of the $p-$ port network, which can be synthesized, for whatever set of assigned polynomials (with a finite number of possible exceptions). In case of $p = 2$ (two-port filters), three basic canonical topologies have been widely studied and several methods are well known for the evaluation of the related coupling matrix. These topologies are usually referred as *folded*, *transversal*, and *arrow* [15]. Generally, the synthesis of a canonical prototype can be performed either directly, by using circuital methods (like the one used in Section III for the transversal prototype with $p = 3$), or by means of suitable matrix transformations (the so-called matrix rotations or *Given's* transforms). For two-port filters, [15] shows the sequence of matrix rotations (each defined by an angle and a pivot) producing the coupling matrix of the folded or arrow prototype (the starting matrix is typically the coupling matrix of the transversal prototype, analytically synthesized from the assigned characteristic polynomials). Analyzing the procedure used in [15] for generating the mentioned sequence of rotations, we have devised a general algorithm for building up a family of canonical topologies in case of arbitrary p-port networks. This algorithm is described in the following.

Let $\mathbf{M}$ be the transversal coupling matrix associated to a network with p ports and N nodes (and therefore of order $N + p$). The proposed algorithm is constituted by $N - 1$ sequences of rotations, each depending on one over p possible choices. The number of possible topologies that can be generated is therefore $p^{(N-1)}$, but it should be noted that some of them could be equivalent (i.e., differ only for the nodes and ports numbering). We assume that a specific topology can be identified by assigning a number c in base p, where each figure represents the choice to do at each step of the procedure.

The algorithm is then enunciated as follows:

Assign the starting matrix $\mathbf{M}$
Initialize the vector u as $(1, 2, \ldots, p)$
Transform c into a vector containing its digits
FOR $\mathrm{CT1} = p + 1$ TO $N + p - 1$
  Assign $n = c(\mathrm{CT1} - p) + 1$
    FOR $\mathrm{CT2} = \mathrm{CT1} + 1$ TO $N + p + 3$
      Transform $\mathbf{M}$ with pivot (CT1, CT2) annihilating element $(u(n), \mathrm{CT2})$
    NEXT CT2
  Cancel the element $u(n)$ from vector u and append CT1 to vector u
NEXT CT1

The equations requested for rotating and annihilating specific elements of $\mathbf{M}$ are reported in [15].

Note that the folded and arrow topologies for p-port networks belong to the family of the canonical matrices generated with this algorithm (they are identified, respectively, by $c =$ '$000\ldots0$' and $c =$ '$mmm\ldots m$' with $m = p - 1$). All the others topologies can be considered as intermediate between the mentioned two.

Fig. A1 shows the structures obtained with $p = 3$, $N = 6$ for three different values of c ('00000,' '11111,' and '22222').

Another way to find new topologies by mean of rotations of a canonical matrix is based on the numerical optimization of the rotation angles in a fixed sequence of rotations, spanning all the distinct pivots of the matrix. This procedure was originally introduced in [16] for two-port filters and has been extended here to arbitrary p-port networks. Strictly speaking, it is not said that, for a given sequence of rotations (spanning all the distinct pivots) and a starting canonical matrix, a set of rotation angles always exists that allows the evaluation of the coupling matrix associated to an arbitrary (but realizable) topology. Furthermore, even if these angles exist, the optimization algorithm may fail their determination. On the other hand, the chances for getting the desired goal in the optimization process are greatly increased if many different canonical matrices are available as a starting point. In fact, we have observed that using one of the canonical matrices generated with the previous algorithm as a starting point, the convergence has been always obtained in all the performed tests (in most cases, the optimization was successful starting with the transversal prototype).

It is worth saying that, being that this approach is based on optimization, it is convenient only when the realizability of the desired topology is guaranteed, but there is no algorithm for the analytical determination of the required sequence of matrix rotations.

References

[1] J. D. Rhodes, "Direct design of symmetrical interacting bandpass channel diplexer," *J. Microw., Opt., Acoust.*, vol. I, no. 1, pp. 34–40, Sep. 1976.

[2] A. Morini and T. Rozzi, "Constraints to the optimum performance and bandwidth limitations of diplexers employing symmetric three-port junctions," *IEEE Trans. Microw. Theory Techn.*, vol. 40, no. 2, pp. 242–248, Feb. 1996.

[3] G. Macchiarella and S. Tamiazzo, "Novel approach to the synthesis of microwave duplexers," *IEEE Trans. Microw. Theory Techn.*, vol. 54, no. 12, pp. 4281–4290, Dec. 2006.

[4] S. Shin and S. Kanamaluru, "Diplexer design using EM and circuit simulation techniques," *IEEE Microw. Mag.*, vol. 8, no. 2, pp. 77–82, Apr. 2007.

[5] A. Garcia-Lamperez, M. Salazar-Palma, and T. K. Sarkar, "Analytical synthesis of microwave multiport networks," in *IEEE MTT-S Int. Microw. Symp. Dig.*, Fort Worth, TX, USA, Jun. 2004, pp. 455–458.

[6] A. Garcia-Lamperez and M. Salazar-Palma, "Analytical synthesis of coupling matrices for N-port networks with reactance compensation," presented at the Eur. Microw. Week Workshop on Adv. N-port Netw. Space Appl., Amsterdam, The Netherlands, Oct. 2012.

[7] F. Seyfert, M. Olivi, S. Bila, and H. Ezzeddine, "Nevanlinna pick interpolation and multiplexer synthesis," presented at the Eur. Microw. Week Workshop on Adv. N-port Netw. Space Appl., Amsterdam, Oct. 2012.

[8] R. J. Wenzel, "Application of exact synthesis methods to multichannel filter design," *IEEE Trans. Microw. Theory Techn.*, vol. MTT-13, no. 1, pp. 77–83, Jan. 1965.

[9] G. Matthaei, L. Young, and E. Jones, *Microwave Filters, Impedance-Matching Networks, and Coupling Structures*. Norwood, MA, USA: Artech House, 1980, pp. 165–173, 243–252.

[10] J. D. Rhodes and C. I. Mobbs, "Explicit design of remote-tuned combiner for GSM and WCDMA signals," *Int. J. Circuit Theory Appl.*, vol. 35, pp. 547–564, 2007.

[11] I. C. Hunter, E. Musonda, R. Parry, M. Guess, and M. Meng, "Transversal directional filters for channel combining," in *IEEE MTT-S Int. Microw. Symp. Dig.*, Seattle, WA, USA, Jun. 2013.

[12] R. J. Cameron, C. M. Kudsia, and R. R. Mansour, *Microwave Filters for Communication Systems*. Hoboken, NJ, USA: Wiley, 2007.

[13] R. J. Cameron, C. M. Kudsia, and R. R. Mansour, *Microwave Filters for Communication Systems*. Hoboken, NJ, USA: Wiley, 2007, pp. 304–311.

[14] R. J. Cameron, C. M. Kudsia, and R. R. Mansour, *Microwave Filters for Communication Systems*. Hoboken, NJ, USA: Wiley, 2007, p. 214.

[15] R. J. Cameron, C. M. Kudsia, and R. R. Mansour, *Microwave Filters for Communication Systems*. Hoboken, NJ, USA: Wiley, 2007, pp. , 296, 304, 379.

[16] G. Macchiarella, "Exact synthesis of in-line prototype filters using cascaded triplet and quadruplet sections," *IEEE Trans. Microw. Theory Techn.*, vol. MTT-50, no. 7, pp. 1779–1783, Jul. 2002.